Chemical biology studies on retaining exo-β-glucosidases

Su, Q.

Chapter 2

Xylose-configured cyclophellitols as selective inhibitors for glucocerebrosidase

Taken in part from:

Qin Su, Sybrin P. Schröder, Lindsey T. Lelieveld, Maria J. Ferraz, Marri Verhoek, Rolf G. Boot, Herman S. Overkleeft, Johannes M. F. G. Aerts, Marta Artola, Chi-Lin Kuo, Xylose-configured cyclophellitols as selective inhibitors for glucocerebrosidase, *ChemBioChem,* **2021**, *22*, 3090-3098.

Abstract

Glucocerebrosidase (GBA1), a lysosomal retaining β-D-glucosidase, has recently been shown to hydrolyze β-D-xylosides and to transxylosylate cholesterol. Genetic defects in GBA1 cause the lysosomal storage disorder Gaucher disease (GD), and also constitute a risk factor for developing Parkinson's disease. GBA1 and other retaining glycosidases can be selectively visualized by activity-based protein profiling (ABPP) using fluorescent probes composed of a cyclophellitol scaffold having a configuration tailored to the targeted glycosidase family. GBA1 processes β-D-xylosides in addition to β-D-glucosides, this in contrast to the other two mammalian cellular retaining β-D-glucosidases, GBA2 and GBA3. Here it is shown that the xylopyranose preference also holds up for covalent inhibitors: xylose-configured cyclophellitol and cyclophellitol aziridines selectively react with GBA1 over GBA2 and GBA3 *in vitro* and *in vivo*. As well, it is shown that the xylose-configured cyclophellitol is more potent and more selective for GBA1 than the classical GBA1 inhibitor, conduritol B epoxide (CBE). Both xylose-configured cyclophellitol and cyclophellitol aziridine cause accumulation of glucosylsphingosine in zebrafish embryo, a characteristic hallmark of GD, and it can be concluded that these compounds are well suited for creating such chemically induced GD models.

Introduction

The lysosomal retaining β-D-glucosidase, glucocerebrosidase (GBA1) receives considerable interest given its role in several pathologies.[1] Gaucher disease (GD), an autosomal recessive lysosomal storage disorder, is caused by mutations in the *GBA1* gene that result in reduced lysosomal GBA1 activity. In GD patients, tissue macrophages excessively store in their lysosomes glucosylceramide (GlcCer), an ubiquitous glycosphingolipid.[2] Part of the accumulating GlcCer is converted into glucosylsphingosine (GlcSph) by lysosomal acid ceramidase.[3] The water-soluble GlcSph is able to leave cells and is prominently elevated in plasma and tissues of GD patients.[4] This striking abnormality is exploited for diagnosis.[5-7] Recently, it has been recognized that carriers of mutations in the *GBA1* gene are at an increased risk for developing Parkinson's disease (PD)[8], in which excessive GlcSph is speculated to promote harmful α-synuclein aggregation.[9,10]

The current therapies for the treatment of GD are enzyme supplementation based on chronic intravenous administration of macrophage-targeted human recombinant GBA1, also known as "enzyme replacement therapy", and "substrate reduction therapy" founded on the inhibition of GlcCer synthesis.[11] Gene therapy approaches are presently actively studied in pre-clinical and clinical settings.[12,13] GBA1 has been extensively examined and its life cycle and structural features have been elucidated by various techniques.[1] The catalytic mechanism of GBA1 involves a Koshland double-displacement mechanism in which E340 and E325 serve as nucleophile and acid/base catalytic residues, respectively.[14] Conduritol B epoxide (CBE)[15] reacts with the catalytic nucleophile of GBA1 to form a covalent and irreversible bond, thereby irreversibly inactivating the enzyme,[16,17] and is used extensively in GD[17-20] and PD research.[21-23] Cyclophellitol and its analogues react in the same manner (Figure 1A), but are much more potent GBA1 inhibitors.[16,24] Based on the cyclophellitol scaffold two classes of GBA1-reactive activity-based probes (ABPs) were recently developed: one with the reporter group (fluorophore or biotin) connected via the cyclophellitol O8 and one with the reporter group grafted onto the nitrogen of cyclophellitol aziridine.[25,26] The cyclophellitol-based ABPs react in a highly specific manner with GBA1 and allow its selective and sensitive visualization in organisms and intact cells, even in individual lysosomes.[27,28] The cyclophellitol aziridine-based ABPs on the other hand react with all the cellular retaining β-D-glucosidases: lysosomal GBA1, cytosol-facing, membrane bound GBA2 and cytosolic GBA3.[29]

Recent investigations have revealed that GBA1 is catalytically more versatile than previously considered. Besides hydrolysis of β-D-glucosides, the enzyme catalyses transglucosylation, a process in which glucose is transferred, with retention of anomeric configuration, from GlcCer to an acceptor hydroxyl such as the one in cholesterol.[30,31] In addition, GBA1 hydrolyses β-D-xylosides, including 4-methylumbelliferyl-β-D-xylopyranoside and plant derived β-xylosides like cyanidin-β-xyloside from plums and berries, as well as xylosylceramide.[32] GBA1 is also able to use β-xylosides as donors in transglycosylation reactions, generating xylosylcholesterol and di-xylosylcholesterol, again with retention of configuration with respect to the anomeric centre of the transferred xylose residues.[33] In contrast to GBA1, GBA2 is not active towards β-xylosides and the activity of GBA3 towards these substrates is very low.[33] It thus appears that the presence of the pendant CH_2OH group that distinguishes β-glucosides from β-xylosides is a prerequisite for affinity for GBA2 and GBA3. The flexibility of GBA1 for substrates with a modification at the glucose-C6 is also

reflected by its selective reactivity towards O8-modified cyclophellitol-based inhibitors and ABPs and with those of glucose-C6 modified substrates.[34-37]

In the study described in this chapter, it was examined whether xylose-configured cyclophellitol and cyclophellitol aziridines can react with GBA1, GBA2 and/or GBA3 *in vitro* and *in vivo*, by applying activity-based protein profiling (ABPP) and fluorogenic substrate hydrolysis readouts. These studies reveal that *xylo*-cyclophellitol is a highly effective GBA1 inhibitor that is both more potent and more selective than the widely applied GBA1 inhibitor, CBE.

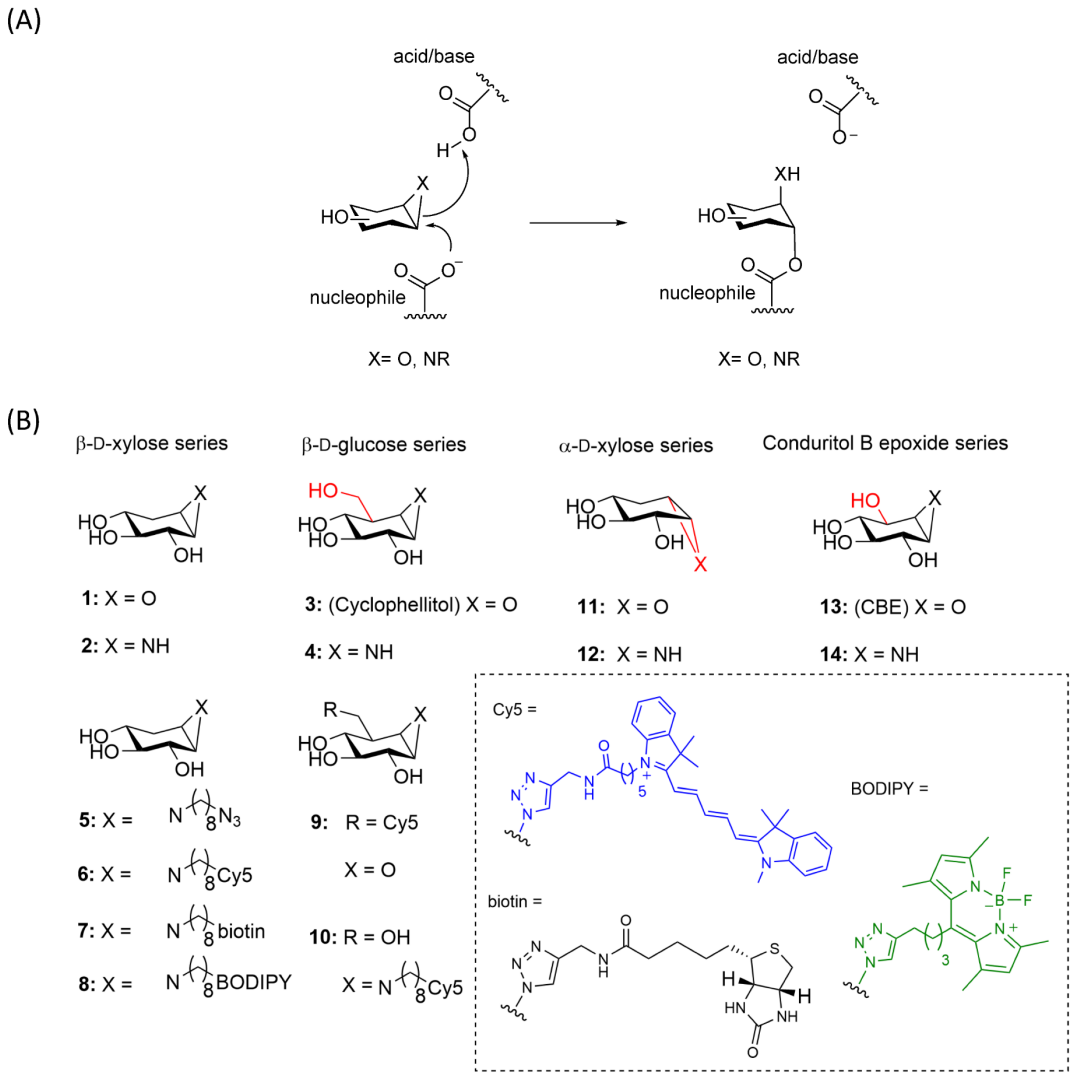

Figure 1. (A) Irreversible inhibition by cyclophellitol and cyclophellitol-aziridine configured compounds. (B) Structures of cyclophellitol configured epoxide and aziridines subject of the research described in this chapter.

Results

In vitro affinity and selectivity of cyclophellitol- and *xylo*-cyclophellitol-based inhibitors and ABPs towards human β-glucosidases

The synthesis of β-*xylo*-cyclophellitol **1**, β-*xylo*-cyclophellitol aziridines **2** and **5** and ABPs **6** and **7**[38,39], cyclophellitol aziridine **4**[40], conduritol B aziridine **14**[40], α-D-xylose-configured cyclophellitol **11** and cyclophellitol aziridine **12** was published previously[38], whereas that of ABP **8** can be found in the appendix and is based on synthetic procedures reported previously.[41]

In the first instance, the inhibitory potency of **1** and **2** for GBA1, GBA2, and GBA3 was assessed by competitive activity-based protein profiling (cABPP). For this, HEK293T cells were generated that contain endogenous GBA1 and overexpressed GBA2 and GBA3. Cell lysates were incubated with **1** or **2** at different concentrations before treatment with the broad-spectrum retaining β-glucosidase ABP **10**.[42] As can be seen in Figure 2, β-*xylo*-cyclophellitol **1** is able to compete ABP labelling of GBA1 but not that of GBA2 or GBA3 at 10-100 μM. β-*Xylo*-cyclophellitol aziridine **2** similarly competes labelling of GBA1 with **10** at lower concentrations (1-10 μM), and also competes ABP labelling of GBA2 at a higher concentration (100 μM). GBA3 was found to be very insensitive towards both compounds, **1** and **2**. GBA1-selectivity was not observed for cyclophellitol **3** nor cyclophellitol aziridine **4** when assessed in the same cABPP assay: both inhibitors block ABP labelling of GBA1 and GBA2 at equal concentrations (0.1-1 μM) (Figure 2) and, though with less potency, also that of GBA3. Compound **5** comprises an extended version of compound **2** bearing an azido-octyl moiety at the aziridine, and it appeared that this hydrophobic extension greatly enhances inhibitory potency against GBA1 and GBA3, but not against GBA2. Conduritol B epoxide **13** (CBE), which is often used to block GBA1 *in situ* or *in vivo*,[18,37,43] showed less GBA1 selectivity: both GBA1 and GBA2 were shown to be inhibited at close concentrations.

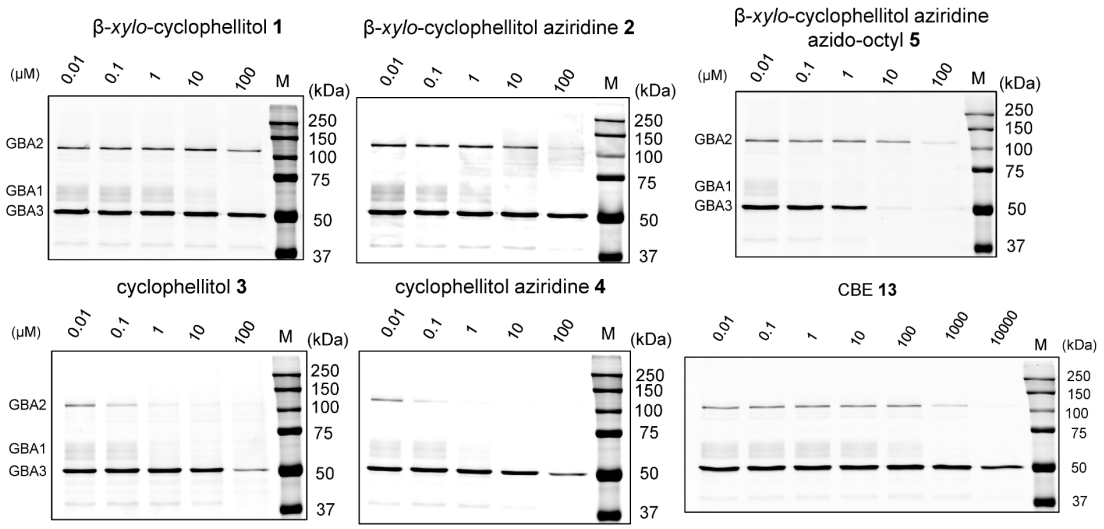

Figure 2. Selectivity of compounds **1**-**5** towards GBA1, GBA2 and GBA3 as visualized by competitive ABPP. Lysates of HEK293T cells expressing human GBA1, GBA2 and GBA3 were incubated with compounds **1**-**5** at indicated concentrations for 30 min, following by treatment with ABP **10**, separation of the denatured protein content by SDS-PAGE and fluorescence scanning of the wet gel slabs.

ABPP was next used to assess the GBA1/GBA2/GBA3 activity and selectivity of β-*xylo*-cyclophellitol aziridine ABPs **6** and **8** in comparison to those of GBA1-selective ABP **9** and ABP **10**. Surprisingly, the labelling pattern of GBA1 and GBA2 with *xylo*-cyclophellitol ABP **6** was very similar to that of the broad-spectrum retaining β-glucosidase ABP **10** (Figure 3): both probes label the two enzymes equally well, while ABP **6** labels GBA3 tenfold less efficiently than ABP **10**. ABP **8** gives a similar labelling pattern of GBA1 and GBA2 but has a higher affinity for GBA3, similar to that of ABP **10** (Figure S4). Cyclophellitol ABP **9** proved to be the most selective ABP towards GBA1 over GBA2 and GBA3, in line with previous results.[36] The unexpected reaction of GBA2 with **6** happens at the catalytic nucleophile (E527) and not at other sites of GBA2, since the GBA2 E527G mutant and the E527G/D677G double mutant did not yield a fluorescent band upon treatment with **6** (Figure 3B). This result is consistent with the observed labelling pattern from the glucose-configured cyclophellitol aziridine ABP **10** (Figure S5).

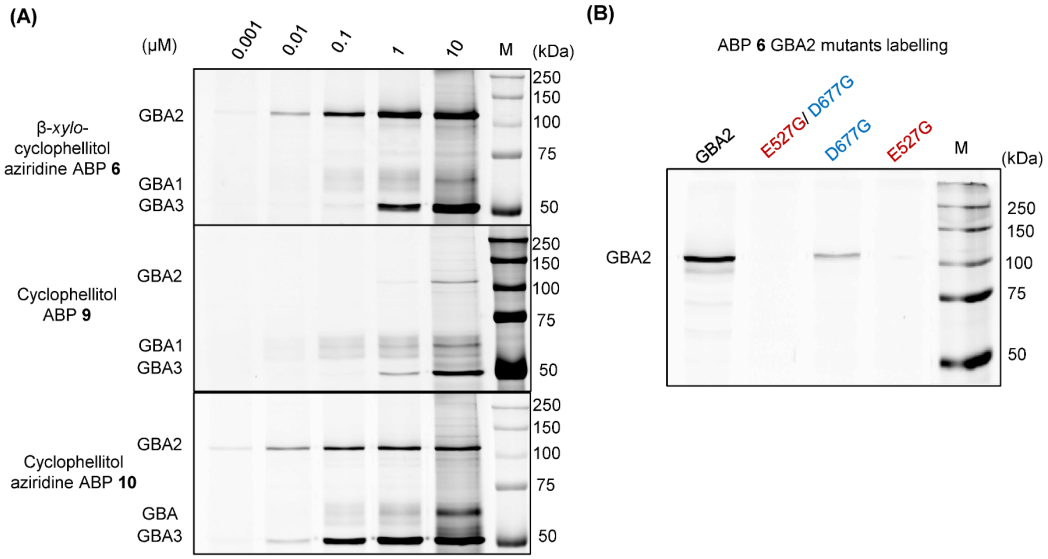

Figure 3. (A) Lysate of HEK293T cells expressing human GBA1, GBA2 and GBA3 was incubated with indicated ABPs (**6**, **9** or **10**) for 30 min at pH 6.0. ABP-reacted proteins were visualized after SDS-PAGE by fluorescence scanning of the wet gel slabs. (B) Labelling with ABP **6** of wild type, catalytic nucleophile mutant (E527G), catalytic acid/base mutant (D677G) or double (E527G/D677G) mutant GBA2 in HEK293T cell extracts.

Apparent IC_{50} values for *xylo*-cyclophellitols (**1**, **2**, **5**-**8**), in comparison with *Glc*-cyclophellitols (**3**, **4**), as inhibitors of GBA1, GBA2 and GBA3 were next determined in fluorogenic substrate assays as follows. Either recombinant, isolated GBA1 (imiglucerase), lysate of GBA1/GBA2 knockout (KO) HEK293T cells overexpressing GBA2, or lysate of GBA1/GBA2 KO cells overexpressing GBA3 were incubated for 30 min with varying concentrations of each of the inhibitors **1**-**14** followed by treatment with the fluorogenic substrate, 4-methylumbelliferyl-β-D-glucopyranoside (4-MU-β-D-Glc) and fluorescence readout. In agreement with the cABPP results, compounds **1** and **2** proved to be potent inhibitors of GBA1 (apparent IC_{50} of 2671 nM and 719 nM respectively) while only modestly inhibiting GBA2 and GBA3 (apparent IC_{50} > 25 μM), whereas cyclophellitol **3** and aziridine **4** are

equally potent against GBA1 and GBA2.[44] A somewhat decreased potency against GBA3 was also noted from **1** and **2** over **3** and **4**, consistent with the cABPP results. *N*-octyl *xylo*-cyclophellitol aziridine **5** proved to be a much more potent GBA1 and GBA3 inhibitor with 600-fold increased potency for GBA1 and over 40-fold increased potency for GBA3, when compared to the unsubstituted *xylo*-cyclophellitol aziridine **2**. In contrast, its potency as GBA2 inhibitor proved to be only five-fold higher than that of **2** (Table 1). Compound **5** is therefore an even more GBA1-selective inhibitor *in vitro* when compared to **2** (IC_{50} ratio GBA2/GBA1 = 5317, GBA3/GBA1 = 486). The *xylo*-cyclophellitol aziridine ABPs **6**-**8** also selectively inhibit GBA1 over GBA2 and GBA3, but their selectivity window between GBA1 and GBA2 is less than that of **5**.[45] Neither α-D-*xylo*-configured epoxide **11** nor aziridine **12** show significant inhibition of either of the three retaining β-glucosidases (Table S1), in contrast to the observed affinity of α-glucose configured cyclophellitol aziridines, both of which have been shown to react with GBA1 and GBA2.[39]

Table 1. *In vitro* apparent IC_{50} values (nM) of compounds **1**-**8** and **13** towards β-glucosidases rhGBA1, GBA2 and GBA3. Apparent IC_{50} values were derived from the average of three individual experiments as measured by enzymatic assays using 4-MU-β-D-Glc as the fluorogenic substrate. Inhibitors were incubated with enzymes for 30 min, following addition of 4-MU-β-D-Glc for 30 min incubation. Error ranges = ± SD, n = 3 replicates.

inhibitors	rhGBA1[a]	GBA2[b]	GBA3[c]	(Ratio) GBA2/ GBA1	(Ratio) GBA3/ GBA1
1	2671 ± 94.5	> 5×10^4	> 5×10^4	> 19	> 19
2	719 ± 196	31587 ± 926	> 2.5×10^4	44	> 35
3 (CP)	400 ± 12.4	148 ± 7.51	51499 ± 4013	0.4	129
4	341 ± 5.82	279± 44.5	33817 ± 2428	0.8	99
5	1.20 ± 0.06	6380 ± 1155	583 ± 202	5317	486
6	6.44 ± 0.49	544 ± 110	10055 ± 1003	84	1561
7	164 ± 22.1	48270 ± 9014	25267 ± 5007	295	155
8	2.70 ± 0.45	61.2 ± 12.0	522 ± 209	23	193
13 (CBE)	34902 ± 1668	> 5×10^5	> 5×10^5	> 14	> 14

[a]rhGBA1 = isolated, recombinant human GBA1 (Imiglucerase). [b]GBA2 = lysate of GBA1/GBA2 KO HEK293T cells with GBA2 overexpression. [C]GBA3 = lysate of GBA1/GBA2 KO HEK293T cells with GBA3 overexpression.

Affinity and selectivity of xylose-configured cyclophellitol epoxide 1 and aziridine 2 towards human β-glucosidases *in vivo*

The activity of **1** and **2** towards the three human β-glucosidases in intact HEK293T cells was investigated next. For this experiment, HEK293T cells expressing endogenous GBA1, and overexpressing GBA2 and GBA3 were treated with varying concentrations of **1** or **2** for 24 h, after which lysates were subjected to ABPP using the broad-spectrum β-glucosidase ABP **10**,

followed by SDS-PAGE, fluorescence scanning of the gels and quantification of the fluorescent bands. Compounds **1** and **2** show low IC_{50} values (5.7 nM and 42.2 nM, respectively) for GBA1 and good selectivity for this enzyme relative to GBA2 and GBA3 (Figure 4).

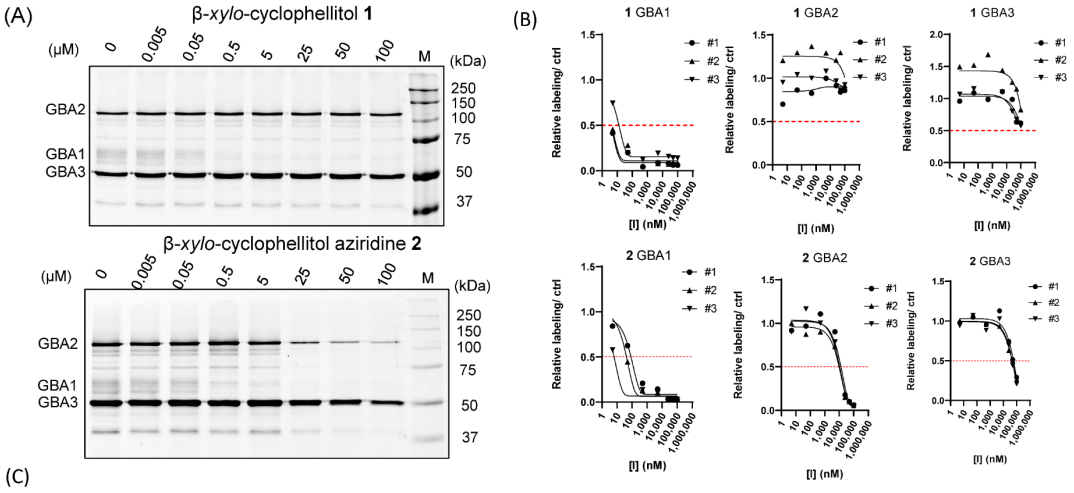

(C)

Intact cells IC_{50}	GBA1	GBA2	GBA3	GBA2/GBA1 ratio	GBA3/GBA1 ratio
1	5.71 ± 3.82 nM	> 1×10^5 nM	> 1×10^5 nM	> 10000	> 10000
2	42.2 ± 38.3 nM	10417 ± 1530 nM	48873 ± 12727 nM	247	1159

Figure 4. Inhibitory effect of β-D-*xylo*-cyclophellitol **1** and β-D-*xylo*-cyclophellitol aziridine **2** on β-glucosidases in intact HEK293T cells expressing endogenous GBA1, and overexpressing GBA2 and GBA3. (A) Representative gel images of cABPP where cells were treated for 24 h with varying concentrations of the indicated inhibitor. Lysates were then prepared and labelled with fluorescent ABP **10**. Fluorescently labelled proteins were visualized after SDS-PAGE (1 set from n = 3 replicates), and IC_{50} values were determined by quantification of fluorescence intensity of the bands. (B) IC_{50} curves (C) IC_{50} values for compounds **1** and **2** as GBA1, GBA2 and GBA3 inhibitors as derived from this cABPP assay.

The affinity of *xylo*-configured cyclophellitols **1** and **2** for retaining β-glucosidases in living animals was then investigated using zebrafish (*Danio rerio*) embryos, which express homologues of both human GBA1 and GBA2. Following exposure for 5 days, fish larvae were sacrificed and lysed, and treatment with ABP **10** was used to detect residual active β-glucosidase molecules in the lysates and for IC_{50} determination. Epoxide **1** selectively abrogates ABP labelling of GBA1 without targeting GBA2 at 150 μM (Figure 5A). Aziridine **2** is also selective against GBA1 over GBA2, albeit with a narrower selectivity window (Figure 5A-C). The apparent IC_{50} in zebrafish embryo is much lower than that observed in intact cells despite the longer incubation time, which could be a result of poor bioavailability of the cyclophellitol-related structures in whole animal, as noted earlier.[37] It was also observed that *xylo*-cyclophellitol **1** has a better GBA1:GBA2 selectivity window over CBE **13** in zebrafish embryo using the same experimental setup, but still do not outperform the previously reported novel GBA1-selective inhibitors based on cyclophellitol functionalized with hydrophobic moieties at C8 (cyclophellitol numbering, the primary carbon corresponding to C6 in glucose).[36] Finally, as revealed by quantification of LC-MS/MS, treatment of zebrafish embryos with compound **1** or **2** in zebrafish embryos led to increased levels of GlcSph (Figure 5D) when compared to non-treated embryos, reflecting functional inactivation of GBA1.

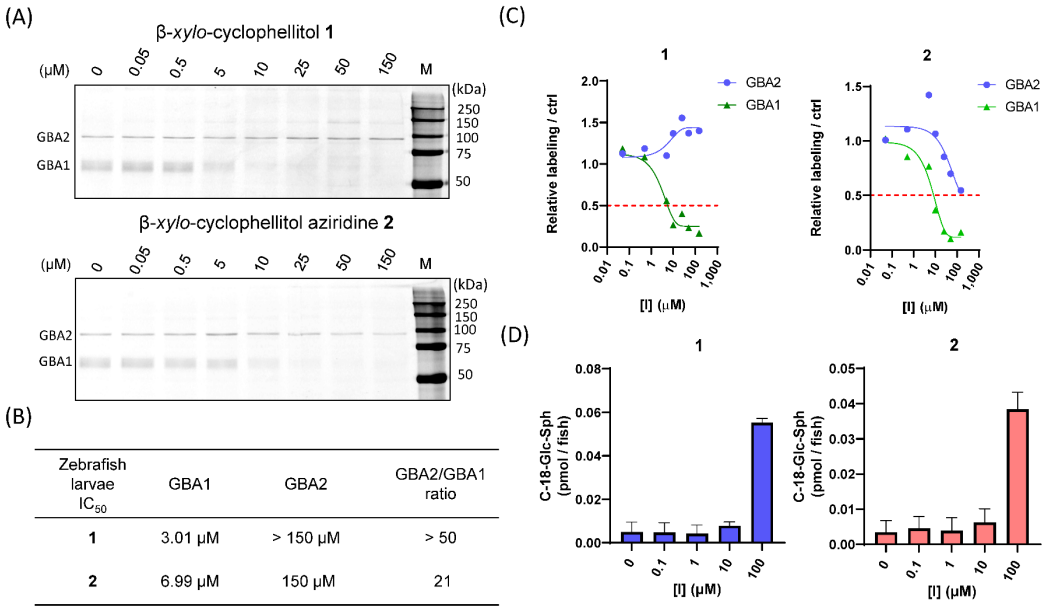

(B)

Zebrafish larvae IC_{50}	GBA1	GBA2	GBA2/GBA1 ratio
1	3.01 μM	> 150 μM	> 50
2	6.99 μM	150 μM	21

Figure 5. *In vivo* inhibitory activity of β-D-*xylo*-cyclophellitol **1** and β-D-*xylo*-cyclophellitol aziridine **2** towards GBA1 and GBA2 in zebrafish (*Danio rerio*) larvae. (A) Larvae were exposed to the indicated inhibitor for 5 days. Larvae were harvested, lysed and incubated with fluorescent ABP **10**. Fluorescently labelled proteins were visualized after SDS-PAGE. (B) Apparent IC_{50} values towards β-glucosidases (GBA1 and GBA2) were determined by fluorescence quantification. (C) *In vivo* inhibition curves. (D) Glucosylsphingosine (GlcSph) levels in zebrafish larvae were determined by quantification of LC-MS/MS, n = 2 replicates.

Comparison of β-D-*xylo*-cyclophellitol (aziridine) and conduritol B epoxide (aziridine)

Prompted by the observation that β-D-*xylo*-cyclophellitol **1** has a better *in vivo* GBA1:GBA2 selectivity profile than CBE (compound **13**), these compounds were compared head-to-head as inhibitors of GBA1 and GBA2 in an *in vitro* setting. For comparison, recombinant, isolated GBA1 (imiglucerase), or lysate of GBA1/GBA2 KO HEK293T cells overexpressing GBA2 were used to incubated with compound **1**, **2**, or **13** for 3 h. In addition, CBE-aziridine **14** was synthesized[38] to allow comparison with β-D-*xylo*-cyclophellitol aziridine **2** in this setting. Using a fluorogenic substrate assay (hydrolysis of 4-MU-β-D-Glc) as readout, a marked increase of potency was observed towards GBA1 for **1** compared to CBE **13**, leading to a seven-fold increase in GBA1:GBA2 selectivity window (as calculated by IC_{50} ratio of GBA2/GBA1, Table 2). *Xylo*-cyclophellitol aziridine **2** also has a slightly larger (three-fold increase) GBA1:GBA2 selectivity window when compared to that of conduritol B aziridine **14** (Table 2), however it is apparent that aziridines **2** and **14** are not as selective towards GBA1 as their epoxide analogues **1** and **13**. In addition, the cABPP assays reveal the poor reactivity of all these compounds towards GBA3 (Figure S3).

Table 2. Inhibition of GBA1 and GBA2 by conduritol B epoxide **13** and aziridine **14** in comparison with β-D-*xylo*-cyclophellitol **1** and aziridine **2**. *In vitro* apparent IC_{50} of **1**, **2**, **13** and **14** as determined by using recombinant GBA1 or lysates of GBA1/GBA2 KO HEK293T cells expressing GBA2. Enzymatic assays were performed for 3 h incubation, n = 3 replicates.

Apparent IC_{50}	Inhibitors	rhGBA1 [a]	GBA2 [b]	GBA2/ GBA1 ratio
In vitro (3 h)	**13**	2.63 ± 0.34 µM	105.3 ± 5.85 µM	40
	14	1.63 ± 0.07 µM	10.79 ± 3.30 µM	6.6
	1	0.45 ± 0.02 µM	122.3 ± 30.20 µM	272
	2	0.24 ± 0.03 µM	5.31 ± 0.12 µM	22

[a] rhGBA1 = recombinant human GBA1, Imiglucerase. [b] GBA2 = lysate of GBA1/GBA2 KO HEK293T cells with GBA2 overexpression.

Discussion

Following the observation that GBA1 is able to hydrolyze β-D-xylosides[33], the question arose whether xylose-configured cyclophellitols can be exploited as GBA1 selective inhibitors. The here-described study reveals that *xylo*-configured cyclophellitol **1** is indeed a potent GBA1 inhibitor that poorly reacts with GBA2 and GBA3 *in vitro*, in intact cells, and in zebrafish larvae. In zebrafish larvae, it functionally inhibits GBA1 as demonstrated by elevated levels of glucosylsphingosine (GlcSph). These data highlight that compound **1** has the required features for the generation of GBA1 chemical knockouts in cells and animals in the context of Gaucher and Parkinson disease research.

The *xylo*-configured cyclophellitol aziridine **2** and its *N*-octyl derivatives **5**-**8** are also all potent GBA1 inhibitors, however their concomitant increase in potency towards GBA2 renders them less GBA1:GBA2 selective compared to *xylo*-cyclophellitol **1**. The labelling of GBA2 by a *xylo*-configured cyclophellitol aziridine **2** is somewhat surprising given the finding that GBA2 does not hydrolyze 4-methylumbelliferyl-β-D-xylopyranoside.[33] Neither the catalytic nucleophile mutant (E527G) nor a combined substitution of catalytic nucleophile and acid/base residue (E527G/D677G) were shown to react, suggesting that the labelling proceeds via the catalytic nucleophile, identical to that of the broad-spectrum β-glucosidase cyclophellitol aziridine ABP **10**.

Finally, it was demonstrated in a head-to-head comparison that xylose-configured cyclophellitol **1** is more potent and selective against GBA1 than conduritol B epoxide (CBE, **13**), which is the compound commonly used to generate chemical knockdown GD models in cells and even organisms such as mice.[18,37,43] *Xylo*-cyclophellitol aziridine **2** is similarly more potent and selective against GBA1 than conduritol aziridine **14**, again demonstrating the superiority of the *xylo*-configuration over the CBE configuration in terms of GBA1 selectivity. *Xylo*-cyclophellitol **1** may therefore be a suitable compound for generating improved chemical GBA1 knockout cells and animal models for the study of Gaucher disease and Parkinson's disease.

Experimental procedures

Materials

Recombinant human GBA1 (rhGBA1, Imiglucerase) was obtained from Sanofi Genzyme (Cambridge, MA, USA). 4-Methylumbelliferyl-β-D-glucopyranoside was purchased from Glycosynth (Warrington Cheshire, UK). HEK293T (CRL-3216™) cells were purchased from ATCC (Manassas, VA, USA), and cultured in DMEM medium (Sigma-Aldrich), supplied with 10% (v/v) FCS, 0.1% (w/v) penicillin/streptomycin and 1% (v/v) Glutamax, at 37°C under 7% CO_2. Zebrafish (strain AB/TL) were housed at Leiden University, The Netherlands, and maintained and handled in compliance with the directives of the local animal welfare committee (Instantie voor Dierwelzijn, Leiden) and guidelines specified by the EU Animal Protection Directive 2010/63/EU. Polytron PT 1300D sonicator (Kinematica, Luzern, Switzerland) and potassium phosphate buffer (25 mM KH_2PO_4-K_2HPO_4, pH 6.5, supplemented with protease inhibitor cocktail (EDTA-free, Roche, Basel, Switzerland) and 0.1% (v/v) Triton X-100) were used for lysing cells and homogenizing zebrafish larvae. Protein concentration was measured using the Pierce BCA assay kit (Thermo Fisher Scientific, Waltham, MA, USA). Harvested cells (cell pellets) and cell lysates not used directly were stored at -80 °C.

Cyclophellitol and xylose-configured inhibitors and ABPs **1**, **2**, **11** and **12**[38]; **4** and **14**[26]; **5**, **6** and **7**[46]; **3**, **9**, **10** and **13**[39,47] were synthesized as described in the literature. Synthetic methods and NMR characterization of compound **8** can be found in the appendix (Scheme S1). Chemicals were obtained from Sigma-Aldrich (St. Louis, MO, USA) if not otherwise indicated. Conduritol B epoxide (CBE) was purchased from Enzo Life Sciences (Farmingdale, NY, USA).

Generation of cells genetically modified in β-glucosidase expression

For overexpression of the different β-glucosidases, use was made of HEK293T cells lacking both GBA1 and GBA2. To this end the CRISPR/Cas9 system and the PX330 plasmid were used in order to generate knockout HEK293T cells for both GBA1 and GBA2 genes in these cells.[48] First the GBA1 knockout cells were generated using the annealed oligonucleotides (top strand: 5'-CACCGCGCTATGAGAGTACACGCAG-3', bottom strand: 5'- AAACCTGCGTGTACTCTCATAGCGC-3') after ligation in the BbsI site of the px330 and subsequent transfection into HEK293T cells. Single cells were created and the different clones were analyzed for lack of expression of GBA1 with enzyme activity assays and ABPP and subsequent genomic sequence analysis. GBA1 knockout cells were next used to create the GBA1/GBA2 double knockout cells using the px330 and the following annealed and ligated oligonucleotides (top strand: 5-CACCGGACGGACTGCTGCAATCCGG-3', bottom strand: 5'-AAACCCGGATTGCAGCAGTCCGTCC-3'). Double GBA1/GBA2 knockout cells were selected using fluorogenic substrate and ABPP assays and used for transfection with either human GBA2 or human GBA3 constructs. The design of cloning primers was based on NCBI reference sequences NM_020944.2 for human GBA2 and NM_020973.3 for human GBA3.

The HEK293T cells with either overexpressed GBA2 or GBA3 (in the GBA1/GBA2 KO background) were generated for 4MU fluorogenic assays as described below. GBA1/2 KO HEK293T cells with GBA2 overexpression were generated by transfecting the double GBA1 and GBA2 gene knockout HEK293T cells with human GBA2 constructs. GBA1/2 KO HEK293T cells

with GBA3 overexpression were generated by transfecting the double GBA1 and GBA2 gene knockout HEK293T cells with human GBA3 constructs.

To generate HEK293T cells expressing all cellular β-glucosidases (GBA1, GBA2, and GBA3) for ABPP assays, wild-type HEK293T cells containing endogenous GBA1 and GBA2 were first transfected with human GBA2 constructs to overexpress GBA2, then the GBA1 endogenous and GBA2 overexpressed cells were transfected with human GBA3 constructs to overexpress GBA3.

HEK293T cells expressing GBA2-E527G, GBA2-D677G, or GBA2-E527G/D677G mutants were generated as described previously for COS-7 cells.[49]

Cell lysis

HEK293T cells were cultured with the method described above to 80-90% confluency, and were detached from the culture dishes by trypsin treatment after which some DMEM medium was added. The cells were collected by pipetting and DMEM medium was removed by centrifuging. The cells were washed 3 times with cold PBS (phosphate-buffered saline), after which they were centrifuged to remove PBS and lysed in potassium phosphate buffer for immediate use by sonication on ice with a sonicator. After sonication, lysed mixtures were centrifuged at 10,000 x *g* for 3 min at 4°C, and the supernatants containing the retaining β-glucosidase activities were used for experiments.

Zebrafish maintaining and homogenization

As earlier described[50], zebrafish embryos and larvae were kept at a constant temperature of 28.5 °C. Embryos and larvae were raised in egg water (60 µg·L−1 sea salt, Sera Marin). Synchronized wild-type ABTL zebrafish embryos were acquired after fertilizing adult female zebrafish (> 3 months old). Larvae were homogenized by using potassium phosphate buffer and a sonicator.

Enzyme activity assays using 4MU fluorogenic substrate

All assays were performed with either recombinant GBA1 or lysates of HEK293T cells or zebrafish larvae in 96-well plates at 37 °C. Samples were diluted with McIlvaine buffer (150 mM citric acid-Na_2HPO_4) to a final volume of 25 µL, at pH appropriate for each enzyme. Assays were performed by incubating the samples with 100 µL 4-methylumbelliferyl-β-D-glucopyranoside substrate diluted in McIlvaine buffer (with 0.1% (w/v) bovine serum albumin (BSA)) for a period of 30 min. The substrate mixtures used for each enzyme were as follows: GBA1: 3.75 mM 4-MU-β-D-glucopyranoside at pH 5.2, supplemented with 0.2% (w/v) sodium taurocholate, 0.1% (v/v) Triton X-100, 0.1% (w/v) bovine serum albumin (BSA); GBA2: 3.75 mM 4 MU-β-D-glucopyranoside at pH 5.8; GBA3: 3.75 mM 4-MU-β-D-glucopyranoside at pH 6.0. After stopping the enzyme reaction with 200 µL 1M NaOH-glycine (pH 10.3), 4-methylumbelliferone fluorescence was measured with a fluorimeter LS55 (Perkin Elmer, Waltham, MA, USA) with λ_{EX} 366 nm and λ_{EM} 445 nm. Enzyme activities were determined by subtraction of the background signal (measured for incubations without enzyme).

The IC_{50} values were determined using fluorogenic substrate assays. For GBA1, 3.16 ng (53 fmol) of rhGBA1 was prepared in 12.5 µL McIlvaine buffer (150 mM, pH 5.2) supplemented

with 0.1 % (v/v) Triton X-100, and 0.2 % (w/v) sodium taurocholate, 0.1% (w/v) bovine serum albumin (BSA). The enzyme was incubated with 12.5 µL of inhibitors diluted in McIlvaine buffer (150 mM, pH 5.2) at 37 °C for 30 min or 3 h. For GBA2, lysate of GBA1/GBA2 KO HEK293T cells overexpressing GBA2 was prepared in 12.5 µL McIlvaine buffer (150 mM, pH 5.8) and incubated with 12.5 µL of inhibitors diluted in McIlvaine buffer (150 mM, pH 5.8) at 37 °C for 30 min or 3 h. For GBA3, lysate of GBA1/GBA2 KO HEK293T cells overexpressing GBA3 was prepared in 12.5 µL McIlvaine buffer (150 mM, pH 6.0) and incubated with 12.5 µL of inhibitors diluted in McIlvaine buffer (150 mM, pH 6.0) at 37 °C for 30 min or 3 h. The enzymatic activities of GBA1, GBA2 and GBA3 were measured as described above. The IC_{50} value was calculated using Graphpad Prism 8.0 with the Nonlinear regression (curve fit) - [Inhibitor] vs. response - Variable slope (four parameters) equation as earlier description.[37]

Activity-based protein profiling (ABPP) with SDS-PAGE

Samples containing GBA1, GBA2 or GBA3 (see above for the exact constitution of these samples) were incubated with excess fluorescent ABPs at optimized conditions. ABPP assays were performed at 37 °C for 30 min if not otherwise stated, in a total sample volume of 20-40 µL and 0.5-1 % final concentration of DMSO. For ABPP of recombinant GBA1 (Imiglucerase), samples containing recombinant GBA1 were treated with either 200 nM β-glucose-configured epoxide ABP **9** or aziridine ABP **10** in McIlvaine buffer (150 mM, pH 5.2, 0.1 % (v/v) Triton X-100, 0.2 % (w/v) sodium taurocholate). For ABPP of samples containing GBA1 and GBA2, such as HEK293T cell lysates containing endogenous GBA1 and overexpressed GBA2, or zebrafish larvae homogenates containing endogenous GBA1 and GBA2, samples were treated with 200 nM ABP **10** in McIlvaine buffer (150 mM, pH 5.8). For ABPP of HEK293T cell lysates containing endogenous GBA1 and overexpressed GBA2/GBA3, samples were treated with 200 nM ABP **10** in McIlvaine buffer (150 mM, pH 6.0). For testing reactivity of β-*xylo*-cyclophellitol aziridine ABP **6** or **8** towards β-glucosidases (GBA1/GBA2/GBA3), ABP **6**, **8** and cyclophellitol configured ABP **9**, **10** (for comparison) with varying concentrations were incubated with HEK293T cell lysates containing endogenous GBA1 and overexpressed GBA2/GBA3 in McIlvaine buffer (150 mM, pH 6.0). For competitive ABPP, HEK293T cell lysates containing endogenous GBA1 and overexpressed GBA2/GBA3 were first treated with inhibitors (**1**-**5**, **13**, **14**) in McIlvaine buffer (150 mM, pH 6.0), following incubation with ABP **10** to reveal residual active β-glucosidases. After incubation with ABP, samples were boiled in 5× Laemmli buffer (50 % (v/v) 1 M Tris-HCl, pH 6.8, 50 % (v/v) 100 % glycerol, 10 % (w/v) DTT, 10 % (w/v) SDS, 0.01 % (w/v) bromophenol blue) for 5 min at 98 °C, and separated by gel electrophoresis on 10 % (w/v) SDS-PAGE gels running continuously at 90V for 1-1.5 h. Wet gel slabs were scanned for fluorescence using the Typhoon FLA 9500 (GE Healthcare) at λ_{EX} 473 nm and $\lambda_{EM} \geq$ 510 nm for fluorescent ABP **8**; and at λ_{EX} 635 nm and $\lambda_{EM} \geq$ 665 nm for fluorescent ABP **6**, **9** and **10**. ABP-emitted fluorescence was quantified using ImageQuant software (GE Healthcare, Chicago, IL, USA) and curve-fitted using Prism 8.0 (GraphPad Software). After fluorescence scanning, SDS-PAGE gels were stained for loading control of proteins with Coomassie G250 and scanned on a ChemiDoc MP imager (Bio-Rad, Hercules, CA, USA).[25]

Assessment of inhibitor activity in cultured cells

Confluent HEK293T expressing human GBA1 and overexpressing both GBA2 and GBA3 were cultured in 24-well plates in triplicates with or without inhibitors for 24 h at 37 °C under 7% CO_2. Next, cells were washed three times with PBS, subsequently lysed in potassium phosphate buffer (with 2.5 U/ mL Benzonase® nuclease), the thus obtained samples were incubated for 30 min on ice (for degradation of DNA and RNA by Benzonase® nuclease), aliquoted, and used. After determination of the protein concentration, lysates containing equal protein amount (4−8 µg total protein per measurement) were adjusted to 4 µL with potassium phosphate buffer and subjected to residual activity measurements and/or detection of remaining active enzyme molecules using ABP labelling (n = 3 biological replicates).

Inhibition of enzymes in zebrafish larvae

Experiments were performed with 5 dpf (days post fertilization) larvae. For inhibitor treatment, a single fertilized embryo was seeded in a well of a 96-wells plate and exposed to 200 µL inhibitor with varying concentrations in egg water (60 µg·L−1 sea salt) for 115 hours at 28.5 °C. Per condition, n = 24 embryos were used. At 115 hours, larvae were collected, rinsed three times with egg water, fully aspirated, snap-frozen in liquid nitrogen and homogenized in 96 µL 25 mM potassium phosphate buffer per 24 individuals. Lysis was conducted by sonication on ice with a sonicator at 20% power, three times for three seconds. Samples containing 5-20 µg total protein were used for ABPP assays.

Sphingolipid extraction and analysis by mass spectrometry in inhibitor treated zebrafish larvae

Zebrafish embryos were seeded in 96-well plates (1 fish embryo/well, 200 µL egg water/well) and treated with inhibitors at various concentrations for 103 hours at 28.5 °C. Thereafter, zebrafish larvae were washed three times with egg water, and collected in clean snap-cap Eppendorf tubes. Lipids were extracted and measured according to the methods below which were adapted from the literature.[50] Briefly, after removing the supernatant, 20 µL of ^{13}C-GlcSph (0.1 pmol/ μL^{-1} in MeOH), 480 µL MeOH, and 250 µL $CHCl_3$ were added to the sample. The samples were then stirred, left for 30 min at RT, sonicated (5 x 1 min in sonication water bath) and centrifuged for 10 min at 15,700 rpm. Supernatant was collected in a clean tube, and 250 µL $CHCl_3$ and 450 µL 100 mM formate buffer (pH 3.2) were added. The samples were stirred and centrifuged, after which the upper phase was transferred to a clean tube. The lower phase was extracted with 500 µL MeOH and 450 µL formate buffer. The upper phases were pooled and taken to dryness in a vacuum concentrator at 45 °C. The residue was extracted with 700 µL butanol and 700 µL water, stirred and centrifuged. The upper phase (butanol phase) was dried and the residue dissolved in 100 µL MeOH. 10 µL of this sample was used for LC-MS-mediated lipid detection and identification.[51] Two-tailed unpaired t-test was performed in Prism 8.0 software (GraphPad) to determine statistical significance; *p* value <0.05 was considered significant.

References

1. J. M. Aerts, C. L. Kuo, L. T. Lelieveld, D. E. C. Boer, M. J. C. van der Lienden, H. S. Overkleeft and M. Artola, Glycosphingolipids and lysosomal storage disorders as illustrated by gaucher disease, *Curr. Opin. Chem. Biol.*, 2019, **53**, 204-215.
2. J. M. Aerts, M. Artola, M. van Eijk, M. J. Ferraz and R. G. Boot, Glycosphingolipids and infection: potential new therapeutic avenues, *Front. Cell Dev. Biol.*, 2019, **7**, 324.
3. M. J. Ferraz, A. R. Marques, M. D. Appelman, M. Verhoek, A. Strijland, M. Mirzaian, S. Scheij, C. M. Ouairy, D. Lahav, P. Wisse, H. S. Overkleeft, R. G. Boot and J. M. Aerts, Lysosomal glycosphingolipid catabolism by acid ceramidase: formation of glycosphingoid bases during deficiency of glycosidases, *FEBS Lett.*, 2016, **590**, 716-725.
4. N. Dekker, L. van Dussen, C. E. Hollak, H. Overkleeft, S. Scheij, K. Ghauharali, M. J. van Breemen, M. J. Ferraz, J. E. Groener, M. Maas, F. A. Wijburg, D. Speijer, A. Tylki-Szymanska, P. K. Mistry, R. G. Boot and J. M. Aerts, Elevated plasma glucosylsphingosine in Gaucher disease: relation to phenotype, storage cell markers, and therapeutic response, *Blood*, 2011, **118**, 118-127.
5. V. Murugesan, W. L. Chuang, J. Liu, A. Lischuk, K. Kacena, H. Lin, G. M. Pastores, R. Yang, J. Keutzer, K. Zhang and P. K. Mistry, Glucosylsphingosine is a key biomarker of Gaucher disease, *Am. J. Hematol.*, 2016, **91**, 1082-1089.
6. A. Rolfs, A. K. Giese, U. Grittner, D. Mascher, D. Elstein, A. Zimran, T. Bottcher, J. Lukas, R. Hubner, U. Golnitz, A. Rohle, A. Dudesek, W. Meyer, M. Wittstock and H. Mascher, Glucosylsphingosine is a highly sensitive and specific biomarker for primary diagnostic and follow-up monitoring in Gaucher disease in a non-Jewish, Caucasian cohort of Gaucher disease patients, *PLoS One*, 2013, **8**, e79732.
7. M. van Eijk, M. J. Ferraz, R. G. Boot and J. M. Aerts, Lyso-glycosphingolipids: presence and consequences, *Essays Biochem.*, 2020, **64**, 565-578.
8. E. Sidransky, M. A. Nalls, J. O. Aasly, J. Aharon-Peretz, G. Annesi, E. R. Barbosa, A. Bar-Shira, D. Berg, J. Bras, A. Brice, C. M. Chen, L. N. Clark, C. Condroyer, E. V. De Marco, A. Durr, M. J. Eblan, S. Fahn, M. J. Farrer, H. C. Fung, Z. Gan-Or, T. Gasser, R. Gershoni-Baruch, N. Giladi, A. Griffith, T. Gurevich, C. Januario, P. Kropp, A. E. Lang, G. J. Lee-Chen, S. Lesage, K. Marder, I. F. Mata, A. Mirelman, J. Mitsui, I. Mizuta, G. Nicoletti, C. Oliveira, R. Ottman, A. Orr-Urtreger, L. V. Pereira, A. Quattrone, E. Rogaeva, A. Rolfs, H. Rosenbaum, R. Rozenberg, A. Samii, T. Samaddar, C. Schulte, M. Sharma, A. Singleton, M. Spitz, E. K. Tan, N. Tayebi, T. Toda, A. R. Troiano, S. Tsuji, M. Wittstock, T. G. Wolfsberg, Y. R. Wu, C. P. Zabetian, Y. Zhao and S. G. Ziegler, Multicenter analysis of glucocerebrosidase mutations in Parkinson's disease, *N. Engl. J. Med.*, 2009, **361**, 1651-1661.
9. Y. V. Taguchi, J. Liu, J. Ruan, J. Pacheco, X. Zhang, J. Abbasi, J. Keutzer, P. K. Mistry and S. S. Chandra, Glucosylsphingosine promotes alpha-synuclein pathology in mutant GBA-associated Parkinson's disease, *J. Neurosci.*, 2017, **37**, 9617-9631.
10. M. P. Srikanth, J. W. Jones, M. Kane, O. Awad, T. S. Park, E. T. Zambidis and R. A. Feldman, Elevated glucosylsphingosine in Gaucher disease induced pluripotent stem cell neurons deregulates lysosomal compartment through mammalian target of rapamycin complex 1, *Stem Cells Transl. Med.*, 2021, DOI: 10.1002/sctm.20-0386.

11. J. M. Aerts, C. E. Hollak, R. G. Boot, J. E. Groener and M. Maas, Substrate reduction therapy of glycosphingolipid storage disorders, *J. Inherit. Metab. Dis.*, 2006, **29**, 449-456.
12. Phase 1/2 Lentiviral Vector Gene Therapy - The GuardOne Trial of AVR-RD-02 for Subjects With Type 1 Gaucher Disease, https://clinicaltrials.gov/ct2/show/NCT04145037).
13. Phase 1/2 Clinical Trial of PR001 in Infants With Type 2 Gaucher Disease (PROVIDE), https://clinicaltrials.gov/ct2/show/NCT04411654).
14. C. L. Kuo, E. van Meel, K. Kytidou, W. W. Kallemeijn, M. Witte, H. S. Overkleeft, M. Artola and J. M. Aerts, Activity-based probes for glycosidases: profiling and other applications, *Methods Enzymol.*, 2018, **598**, 217-235.
15. S. Atsumi, C. Nosaka, H. Iinuma and K. Umezawa, Inhibition of glucocerebrosidase and induction of neural abnormality by cyclophellitol in mice, *Arch. Biochem. Biophys.*, 1992, **297**, 362-367.
16. M. D. Witte, W. W. Kallemeijn, J. Aten, K. Y. Li, A. Strijland, W. E. Donker-Koopman, A. M. van den Nieuwendijk, B. Bleijlevens, G. Kramer, B. I. Florea, B. Hooibrink, C. E. Hollak, R. Ottenhoff, R. G. Boot, G. A. van der Marel, H. S. Overkleeft and J. M. Aerts, Ultrasensitive in situ visualization of active glucocerebrosidase molecules, *Nat. Chem. Biol.*, 2010, **6**, 907-913.
17. L. Premkumar, A. R. Sawkar, S. Boldin-Adamsky, L. Toker, I. Silman, J. W. Kelly, A. H. Futerman and J. L. Sussman, X-ray structure of human acid-beta-glucosidase covalently bound to conduritol-B-epoxide. Implications for Gaucher disease, *J. Biol. Chem.*, 2005, **280**, 23815-23819.
18. A. Vardi, H. Zigdon, A. Meshcheriakova, A. D. Klein, C. Yaacobi, R. Eilam, B. M. Kenwood, A. A. Rahim, G. Massaro, A. H. Merrill, Jr., E. B. Vitner and A. H. Futerman, Delineating pathological pathways in a chemically induced mouse model of Gaucher disease, *J. Pathol.*, 2016, **239**, 496-509.
19. Y. Kacher, B. Brumshtein, S. Boldin-Adamsky, L. Toker, A. Shainskaya, I. Silman, J. L. Sussman and A. H. Futerman, Acid beta-glucosidase: insights from structural analysis and relevance to Gaucher disease therapy, *Biol. Chem.*, 2008, **389**, 1361-1369.
20. L. G. Kanfer, J. Sullivan, S. S. Raghavan and R. A Mumford, The Gaucher mouse, *Biochem. Biophys. Res. Commun.,* 1975, **67**, 85–90.
21. A. B. Manning-Bog, B. Schule and J. W. Langston, Alpha-synuclein-glucocerebrosidase interactions in pharmacological Gaucher models: a biological link between Gaucher disease and parkinsonism, *Neurotoxicology*, 2009, **30**, 1127-1132.
22. Y. H. Xu, Y. Sun, H. Ran, B. Quinn, D. Witte and G. A. Grabowski, Accumulation and distribution of alpha-synuclein and ubiquitin in the CNS of Gaucher disease mouse models, *Mol. Genet. Metab.*, 2011, **102**, 436-447.
23. E. M. Rocha, G. A. Smith, E. Park, H. Cao, A. R. Graham, E. Brown, J. R. McLean, M. A. Hayes, J. Beagan, S. C. Izen, E. Perez-Torres, P. J. Hallett and O. Isacson, Sustained systemic glucocerebrosidase inhibition induces brain alpha-synuclein aggregation, microglia and complement C1q activation in mice, *Antioxid. Redox Signal.*, 2015, **23**, 550-564.

24. S. G. Withers and K. Umezawa, Cyclophellitol: A naturally occurring mechanism-based inactivator of beta-glucosidases, *Biochem. Biophys. Res. Commun.*, 1991, **177**, 532-537.
25. W. W. Kallemeijn, K. Y. Li, M. D. Witte, A. R. Marques, J. Aten, S. Scheij, J. Jiang, L. I. Willems, T. M. Voorn-Brouwer, C. P. van Roomen, R. Ottenhoff, R. G. Boot, H. van den Elst, M. T. Walvoort, B. I. Florea, J. D. Codée, G. A. van der Marel, J. M. Aerts and H. S. Overkleeft, Novel activity-based probes for broad-spectrum profiling of retaining beta-exoglucosidases in situ and in vivo, *Angew. Chem. Int. Ed.*, 2012, **51**, 12529-12533.
26. L. Wu, Z. Armstrong, S. P. Schröder, C. de Boer, M. Artola, J. M. Aerts, H. S. Overkleeft and G. J. Davies, An overview of activity-based probes for glycosidases, *Curr. Opin. Chem. Biol.*, 2019, **53**, 25-36.
27. D. Herrera Moro Chao, W. W. Kallemeijn, A. R. Marques, M. Orre, R. Ottenhoff, C. van Roomen, E. Foppen, M. C. Renner, M. Moeton, M. van Eijk, R. G. Boot, W. Kamphuis, E. M. Hol, J. Aten, H. S. Overkleeft, A. Kalsbeek and J. M. Aerts, Visualization of active glucocerebrosidase in rodent brain with high spatial resolution following *in situ* labeling with fluorescent activity based probes, *PLoS One*, 2015, **10**, e0138107.
28. E. van Meel, E. Bos, M. J. C. van der Lienden, H. S. Overkleeft, S. I. van Kasteren, A. J. Koster and J. M. Aerts, Localization of active endogenous and exogenous beta-glucocerebrosidase by correlative light-electron microscopy in human fibroblasts, *Traffic*, 2019, **20**, 346-356.
29. W. W. Kallemeijn, K. Y. Li, M. D. Witte, A. R. Marques, J. Aten, S. Scheij, J. Jiang, L. I. Willems, T. M. Voorn-Brouwer, C. P. van Roomen, R. Ottenhoff, R. G. Boot, H. van den Elst, M. T. Walvoort, B. I. Florea, J. D. Codée, G. A. van der Marel, J. M. Aerts and H. S. Overkleeft, Novel activity-based probes for broad-spectrum profiling of retaining beta-exoglucosidases in situ and in vivo, *Angew. Chem. Int. Ed.*, 2012, **51**, 12529-12533.
30. H. Akiyama, S. Kobayashi, Y. Hirabayashi and K. Murakami-Murofushi, Cholesterol glucosylation is catalyzed by transglucosylation reaction of beta-glucosidase 1, *Biochem. Biophys. Res. Commun.*, 2013, **441**, 838-843.
31. A. R. Marques, M. Mirzaian, H. Akiyama, P. Wisse, M. J. Ferraz, P. Gaspar, K. Ghauharali-van der Vlugt, R. Meijer, P. Giraldo, P. Alfonso, P. Irun, M. Dahl, S. Karlsson, E. V. Pavlova, T. M. Cox, S. Scheij, M. Verhoek, R. Ottenhoff, C. P. van Roomen, N. S. Pannu, M. van Eijk, N. Dekker, R. G. Boot, H. S. Overkleeft, E. Blommaart, Y. Hirabayashi and J. M. Aerts, Glucosylated cholesterol in mammalian cells and tissues: formation and degradation by multiple cellular beta-glucosidases, *J. Lipid Res.*, 2016, **57**, 451-463.
32. D. E. C. Boer, M. Mirzaian, M. J. Ferraz, A. Nadaban, A. Schreuder, A. Hovnanian, J. van Smeden, J. A. Bouwstra and J. M. Aerts, Glucosylated cholesterol in skin: synthetic role of extracellular glucocerebrosidase, *Clin. Chim. Acta.*, 2020, **510**, 707-710.
33. D. E. Boer, M. Mirzaian, M. J. Ferraz, K. C. Zwiers, M. V. Baks, M. D. Hazeu, R. Ottenhoff, A. R. A. Marques, R. Meijer, J. C. P. Roos, T. M. Cox, R. G. Boot, N. Pannu, H. S. Overkleeft, M. Artola and J. M. Aerts, Human glucocerebrosidase mediates formation of xylosyl-cholesterol by beta-xylosidase and transxylosidase reactions, *J. Lipid Res.*, 2021, **62**, 100018.
34. R. A. Ashmus, D. L. Shen and D. J. Vocadlo, Fluorescence-quenched substrates for quantitative live cell imaging of glucocerebrosidase activity, *Methods Enzymol.*, 2018, **598**, 199-215.

35. M. C. Deen, C. Proceviat, X. Shan, L. Wu, D. L. Shen, G. J. Davies and D. J. Vocadlo, Selective fluorogenic beta-glucocerebrosidase substrates for convenient analysis of enzyme activity in cell and tissue homogenates, *ACS Chem. Biol.*, 2020, **15**, 824-829.
36. M. Artola, C. L. Kuo, L. T. Lelieveld, R. J. Rowland, G. A. van der Marel, J. D. C. Codée, R. G. Boot, G. J. Davies, J. M. Aerts and H. S. Overkleeft, Functionalized cyclophellitols are selective glucocerebrosidase inhibitors and induce a bona fide neuropathic gaucher model in zebrafish, *J. Am. Chem. Soc.*, 2019, **141**, 4214-4218.
37. C. L. Kuo, W. W. Kallemeijn, L. T. Lelieveld, M. Mirzaian, I. Zoutendijk, A. Vardi, A. H. Futerman, A. H. Meijer, H. P. Spaink, H. S. Overkleeft, J. M. Aerts and M. Artola, *In vivo* inactivation of glycosidases by conduritol B epoxide and cyclophellitol as revealed by activity-based protein profiling, *FEBS J.*, 2019, **286**, 584-600.
38. S. P. Schröder, R. Petracca, H. Minnee, M. Artola, J. M. F. G. Aerts, J. D. C. Codée, G. A. van der Marel and H. S. Overkleeft, A divergent synthesis of L-arabino- and D-xylo-configured cyclophellitol epoxides and aziridines, *Eur. J. Org. Chem.*, 2016, **2016**, 4787-4794.
39. J. Jiang, C. L. Kuo, L. Wu, C. Franke, W. W. Kallemeijn, B. I. Florea, E. van Meel, G. A. van der Marel, J. D. C. Codée, R. G. Boot, G. J. Davies, H. S. Overkleeft and J. M. Aerts, Detection of active mammalian GH31 alpha-glucosidases in health and disease using in-class, broad-spectrum activity-based probes, *ACS Cent. Sci.*, 2016, **2**, 351-358.
40. M. Artola, S. Wouters, S. P. Schröder, C. de Boer, Y. Chen, R. Petracca, A. van den Nieuwendijk, J. M. Aerts, G. A. van der Marel, J. D. C. Codée and H. S. Overkleeft, Direct stereoselective aziridination of cyclohexenols with 3-amino-2-(trifluoromethyl)quinazolin-4(3H)-one in the synthesis of cyclitol aziridine glycosidase inhibitors, *Eur. J. Org. Chem.*, 2019, **2019**, 1397-1404.
41. S. P. Schröder, C. de Boer, N. G. S. McGregor, R. J. Rowland, O. Moroz, E. Blagova, J. Reijngoud, M. Arentshorst, D. Osborn, M. D. Morant, E. Abbate, M. A. Stringer, K. Krogh, L. Raich, C. Rovira, J. G. Berrin, G. P. van Wezel, A. F. J. Ram, B. I. Florea, G. A. van der Marel, J. D. C. Codée, K. S. Wilson, L. Wu, G. J. Davies and H. S. Overkleeft, Dynamic and functional profiling of xylan-degrading enzymes in aspergillus secretomes using activity-based probes, *ACS Cent. Sci.*, 2019, **5**, 1067-1078.
42. J. Jiang, W. W. Kallemeijn, D. W. Wright, A. van den Nieuwendijk, V. C. Rohde, E. C. Folch, H. van den Elst, B. I. Florea, S. Scheij, W. E. Donker-Koopman, M. Verhoek, N. Li, M. Schurmann, D. Mink, R. G. Boot, J. D. C. Codée, G. A. van der Marel, G. J. Davies, J. M. Aerts and H. S. Overkleeft, *In vitro* and *in vivo* comparative and competitive activity-based protein profiling of GH29 alpha-l-fucosidases, *Chem. Sci.*, 2015, **6**, 2782-2789.
43. G. Legler, Studies on the action mechanism of glycoside splitting anzymes, I. Presentation and properties of specific inhibitors, *Hoppe-Seyler's Zeitschrift fur Physiologische Chemie*, 1966, **345**, 197-214.
44. M. Artola, L. Wu, M. J. Ferraz, C. L. Kuo, L. Raich, I. Z. Breen, W. A. Offen, J. D. C. Codée, G. A. van der Marel, C. Rovira, J. M. Aerts, G. J. Davies and H. S. Overkleeft, 1,6-Cyclophellitol cyclosulfates: a new class of irreversible glycosidase inhibitor, *ACS Cent. Sci.*, 2017, **3**, 784-793.
45. R. Charoenwattanasatien, S. Pengthaisong, I. Breen, R. Mutoh, S. Sansenya, Y. Hua, A. Tankrathok, L. Wu, C. Songsiriritthigul, H. Tanaka, S. J. Williams, G. J. Davies, G. Kurisu

and J. R. Cairns, Bacterial beta-glucosidase reveals the structural and functional basis of genetic defects in human glucocerebrosidase 2 (GBA2), *ACS Chem. Biol.*, 2016, **11**, 1891-1900.

46. S. P. Schröder, C. de Boer, N. G. S. McGregor, R. J. Rowland, O. Moroz, E. Blagova, J. Reijngoud, M. Arentshorst, D. Osborn, M. D. Morant, E. Abbate, M. A. Stringer, K. Krogh, L. Raich, C. Rovira, J. G. Berrin, G. P. van Wezel, A. F. J. Ram, B. I. Florea, G. A. van der Marel, J. D. C. Codée, K. S. Wilson, L. Wu, G. J. Davies and H. S. Overkleeft, Dynamic and functional profiling of xylan-degrading enzymes in aspergillus secretomes using activity-based probes, *ACS Cent. Sci.*, 2019, **5**, 1067-1078.
47. S. P. Schröder, J. W. van de Sande, W. W. Kallemeijn, C. L. Kuo, M. Artola, E. J. van Rooden, J. Jiang, T. J. M. Beenakker, B. I. Florea, W. A. Offen, G. J. Davies, A. J. Minnaard, J. Aerts, J. D. C. Codée, G. A. van der Marel and H. S. Overkleeft, Towards broad spectrum activity-based glycosidase probes: synthesis and evaluation of deoxygenated cyclophellitol aziridines, *Chem. Commun.*, 2017, **53**, 12528-12531.
48. F. A. Ran, P. D. Hsu, J. Wright, V. Agarwala, D. A. Scott and F. Zhang, Genome engineering using the CRISPR-Cas9 system, *Nat. Protoc.*, 2013, **8**, 2281-2308.
49. W. W. Kallemeijn, M. D. Witte, T. M. Voorn-Brouwer, M. T. Walvoort, K. Y. Li, J. D. C. Codée, G. A. van der Marel, R. G. Boot, H. S. Overkleeft and J. M. Aerts, A sensitive gel-based method combining distinct cyclophellitol-based probes for the identification of acid/base residues in human retaining beta-glucosidases, *J. Biol. Chem.*, 2014, **289**, 35351-35362.
50. L. T. Lelieveld, M. Mirzaian, C. L. Kuo, M. Artola, M. J. Ferraz, R. E. A. Peter, H. Akiyama, P. Greimel, R. van den Berg, H. S. Overkleeft, R. G. Boot, A. H. Meijer and J. Aerts, Role of beta-glucosidase 2 in aberrant glycosphingolipid metabolism: model of glucocerebrosidase deficiency in zebrafish, *J. Lipid Res.*, 2019, **60**, 1851-1867.
51. M. Artola, C. L. Kuo, L. T. Lelieveld, R. J. Rowland, G. A. van der Marel, J. D. C. Codée, R. G. Boot, G. J. Davies, J. Aerts and H. S. Overkleeft, Functionalized cyclophellitols are selective glucocerebrosidase inhibitors and induce a bona fide neuropathic gaucher model in zebrafish, *J. Am. Chem. Soc.*, 2019, **141**, 4214-4218.

Appendix

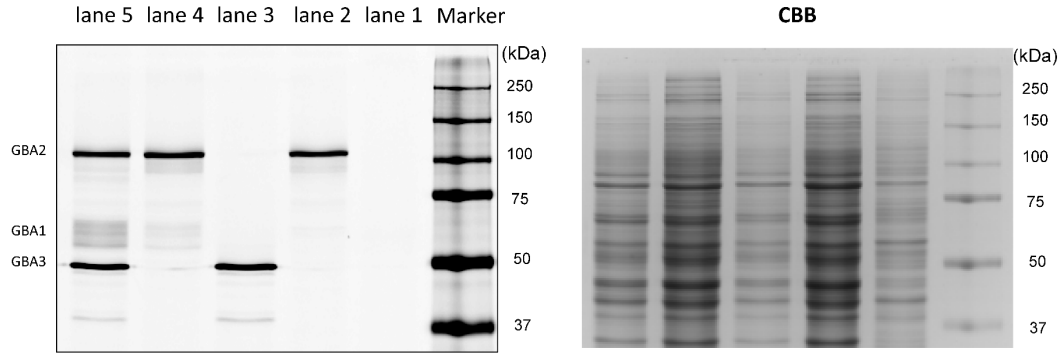

Figure S1. The HEK293T cell line lysates used for experiments. Lane 1, GBA1/GBA2 knock out; Lane 2, GBA1/GBA2 knock out with overexpressed GBA2; Lane 3, GBA1/GBA2 knock out with overexpressed GBA3; Lane 4, GBA1 (endogenous) with overexpressed GBA2; Lane 5, endogenous GBA1 with overexpressed GBA2/GBA3. The cell lysates were incubated with ABP **10** (30 min at pH 6) followed by SDS-PAGE and fluorescent scanning of the gel.

Table S1. *In vitro* apparent IC_{50} of cyclophellitol epoxide ABP **9,** cyclophellitol aziridine ABP **10**, α-*xylo*-configured epoxide **11** and aziridine **12**. The Inhibition curves are showed in Figure S2. [a]rhGBA1 = recombinant human GBA1 (Imiglucerase). [b]GBA2 = lysate of GBA1/GBA2 KO HEK293T cells with GBA2 overexpression. [C] GBA3 = lysate of GBA1/GBA2 KO HEK293T cells with GBA3 overexpression.

in vitro IC_{50}	rhGBA1[a]	GBA2[b]	GBA3[c]	(Ratio) GBA2/ GBA1	(Ratio) GBA3/ GBA1
9	45.20 ± 4.54 nM	> 5 μM	5.78 ± 0.08 μM	> 111	128
10	8.10 ± 1.94 nM	21.5 ± 0.42 nM	8.54 ± 1.18 nM	2.6	1
11	> 50 μM	> 50 μM	> 50 μM	/	/
12	> 50 μM	55.76 ± 2.34 μM	> 50 μM	/	/

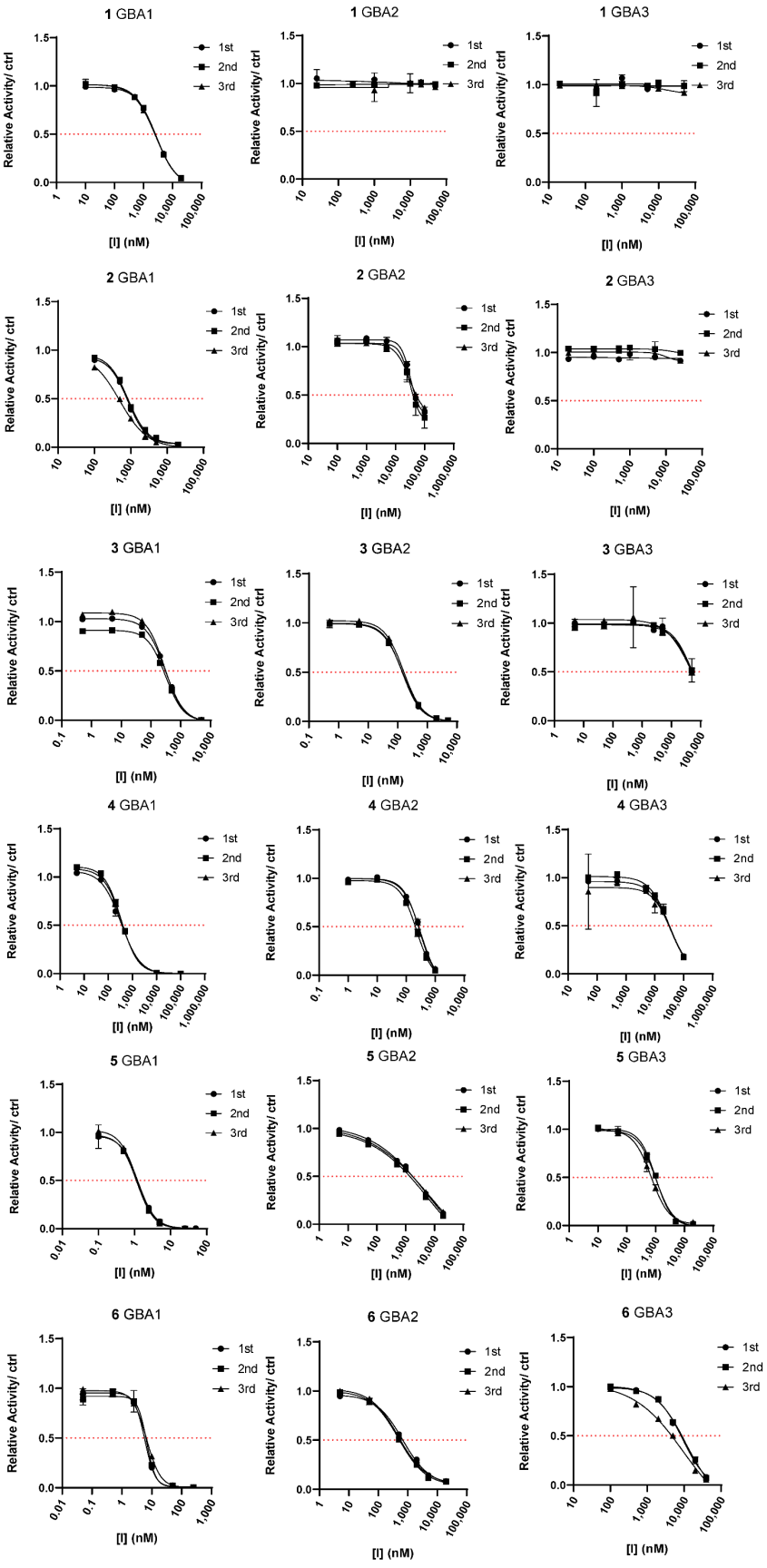

Figure S2 continued (1/3)

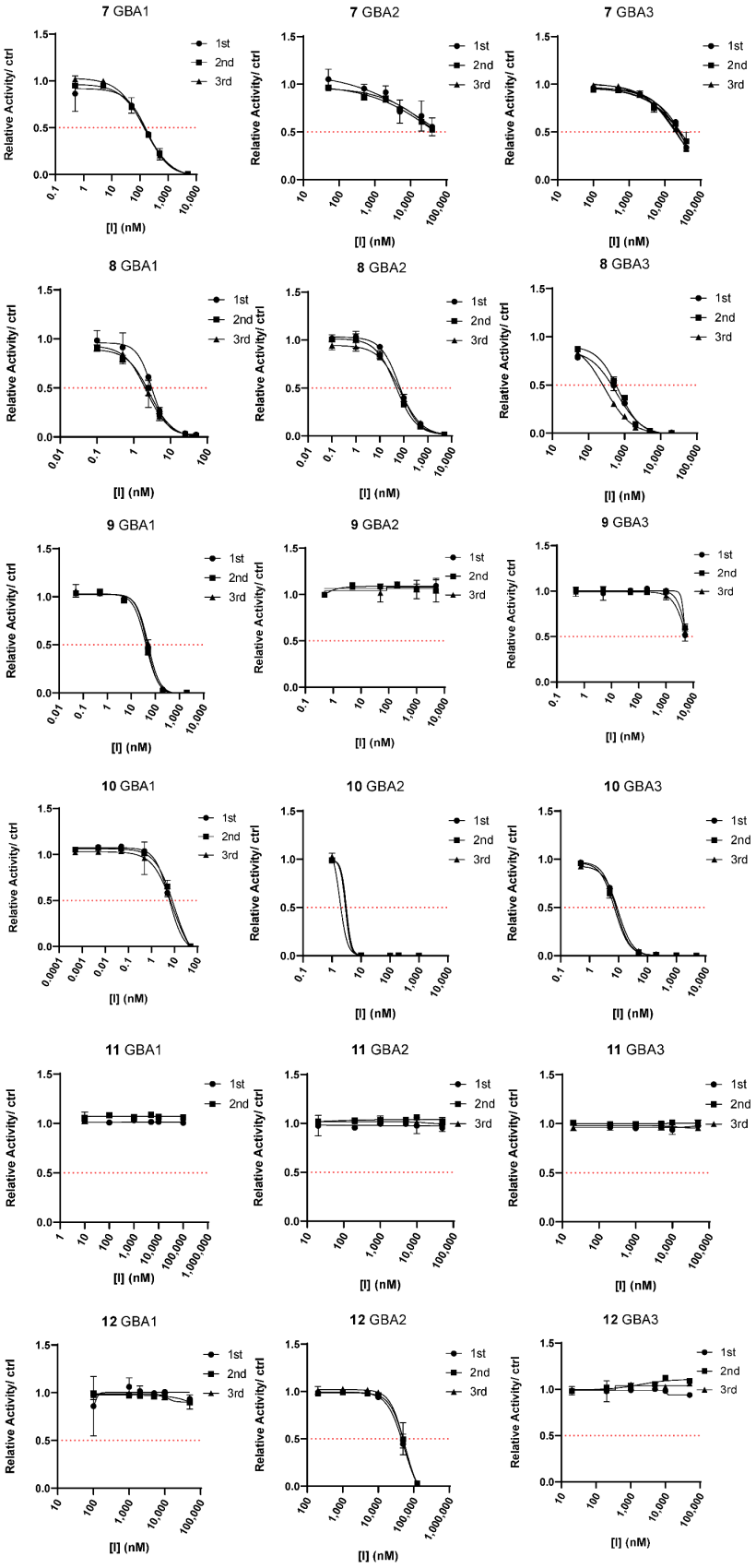

Figure S2 continued (2/3)

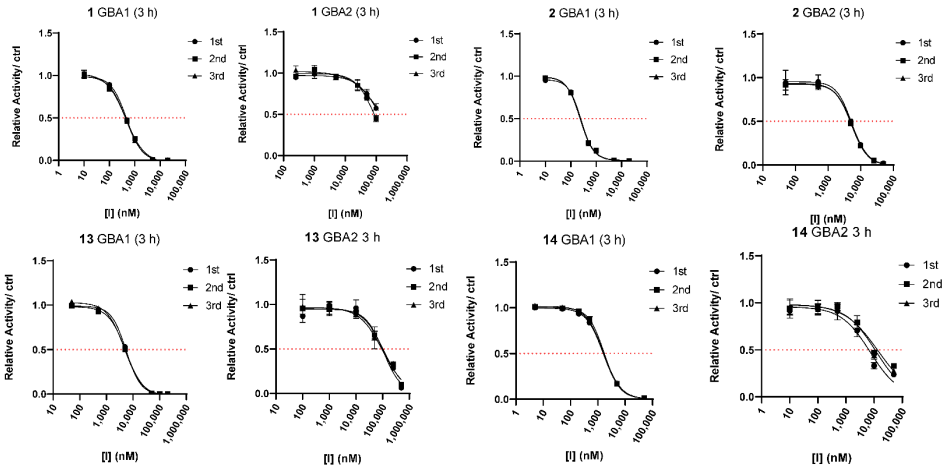

Figure S2. Apparent *In vitro* IC_{50} curves of the different inhibitors (compounds **1**-**14**) as determined by activity measurements after incubation with the inhibitors. The enzymes used were recombinant GBA1 (Imiglucerase), lysates of GBA1/GBA2 KO cells with overexpression of either GBA2 or GBA3. Incubation time for enzyme with the inhibitors is 30 min (if not otherwise stated) or 3 h (marked as '3 h' in figure) at the appropriate pH.

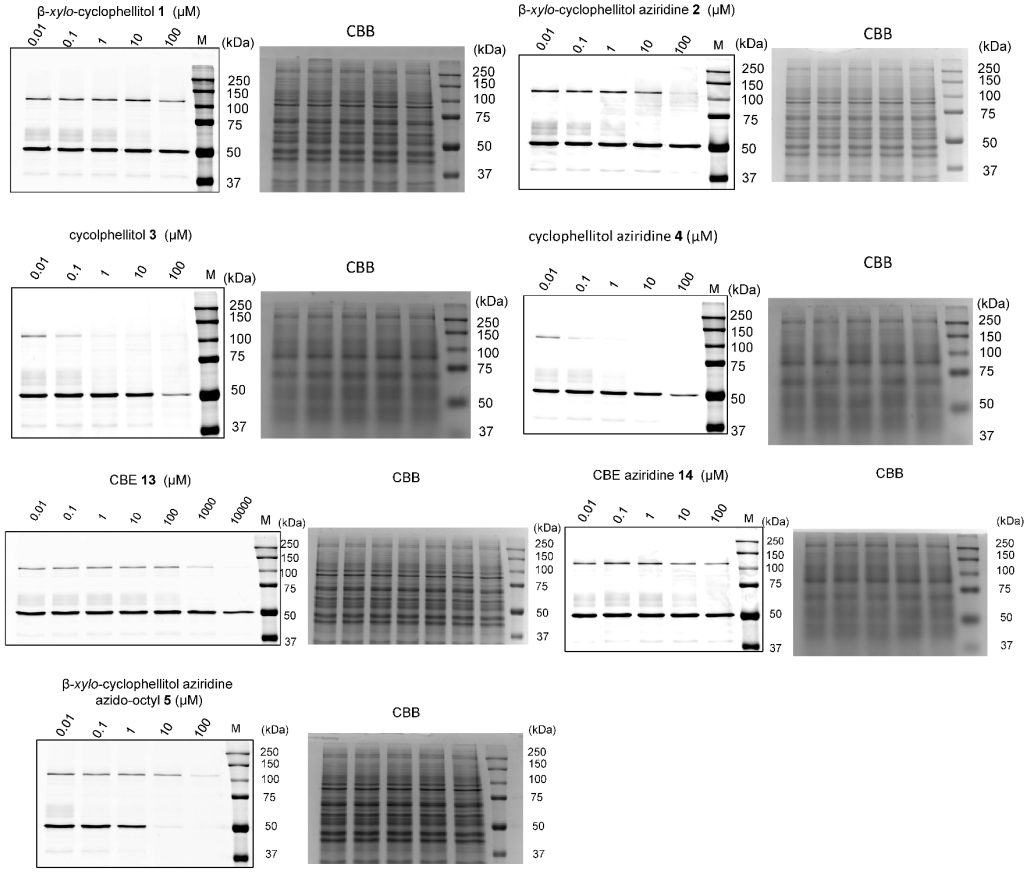

Figure S3. Competitive ABPP assay to visualize the inhibition of compounds (**1**-**5**, **13**, **14**) on HEK293T cell lysates (endogenous GBA1 with overexpressed GBA2/GBA3). Lysates were incubated with inhibitor for 30 min at 37°C *in vitro*, followed by labelling with ABP **10,** SDS-PAGE and fluorescent scanning of the gels. Coomassie brilliant blue staining (CBB) was performed as a loading control.

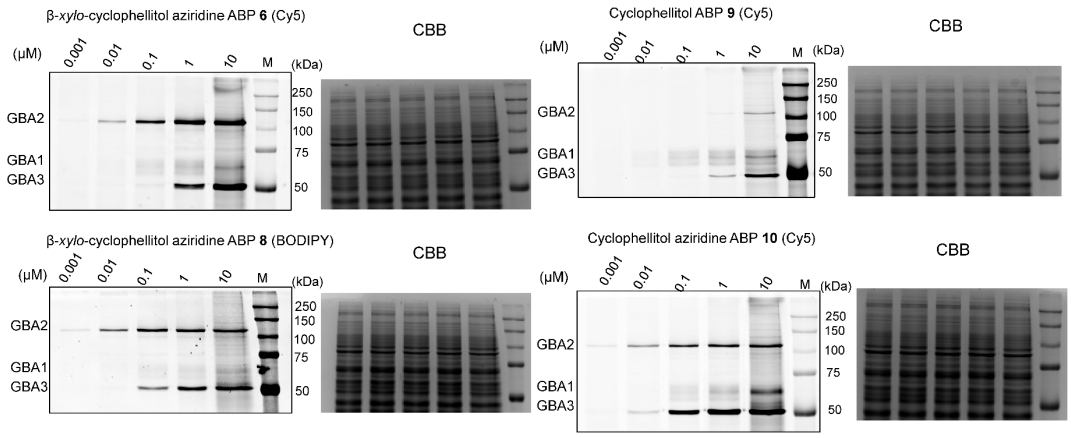

Figure S4. Lysates of HEK293T cells (endogenous GBA1 with overexpressed GBA2/GBA3) were incubated with indicated ABPs (**6**, **8**, **9** or **10**) for 30 min at pH 6.0 *in vitro*. ABP-labelled proteins were visualized after SDS-PAGE by fluorescence scanning of the gels. Coomassie brilliant blue staining (CBB) was performed as a loading control.

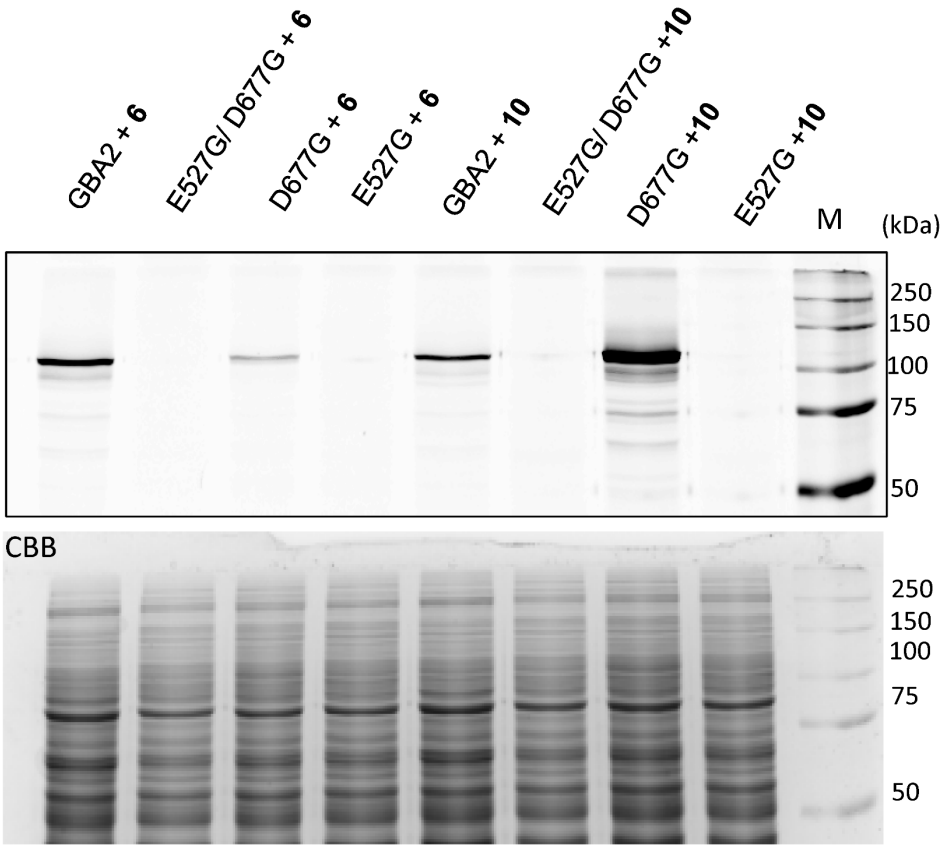

Figure S5. Lysates of HEK293T cells with overexpressed GBA2 variants (either WT, catalytic nucleophile mutant (E527G), catalytic acid/base mutant (D677G) or the double mutant (E527G/D677G)) were incubated with ABP **6** or **10** *in vitro*. ABP-labelled proteins were visualized after SDS-PAGE by fluorescence scanning of the gels. Coomassie brilliant blue staining (CBB) was performed as a loading control.

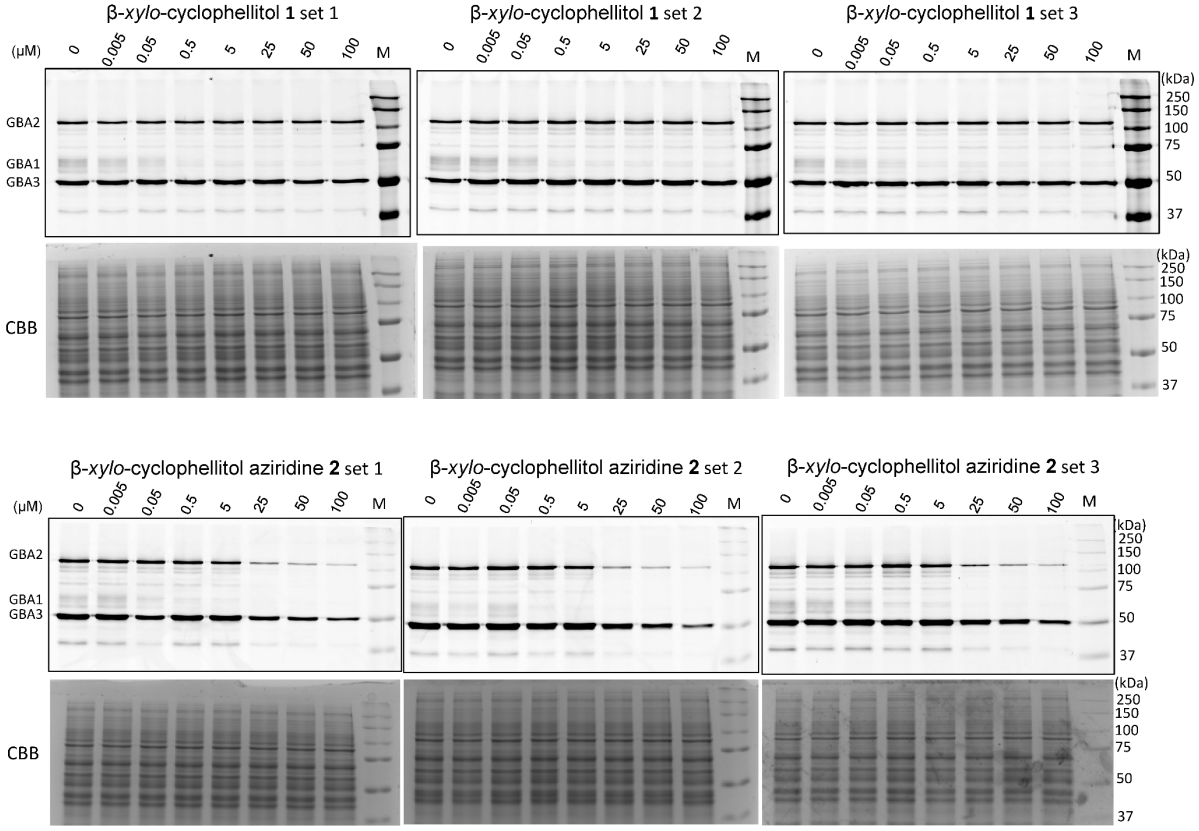

Figure S6. Live cell *in situ* inhibition using β-*xylo*-cyclophellitol epoxide **1** and aziridine **2** in intact HEK293T cells (expressing endogenous GBA1 with overexpressed GBA2/GBA3) for 24 h. After the incubation the cells were harvested and lysed, followed by labelling with ABP **10** *in vitro.* ABP-labelled proteins were visualized after SDS-PAGE by fluorescence scanning of the gels. Coomassie brilliant blue staining (CBB) was performed as a loading control.

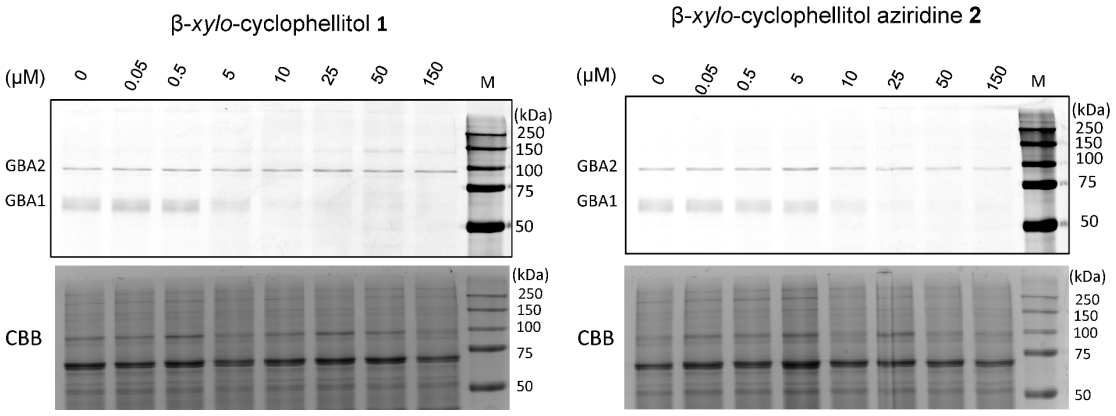

Figure S7. Live zebrafish larvae were incubated with β-*xylo*-cyclophellitol epoxide **1** or aziridine **2** for 5 days *in vivo*. The larvae were harvested, and the homogenate was labelled with ABP **10** *in vitro.* ABP-labelled proteins were visualized after SDS-PAGE by fluorescence scanning of the gels. Coomassie brilliant blue staining (CBB) was performed as a loading control.

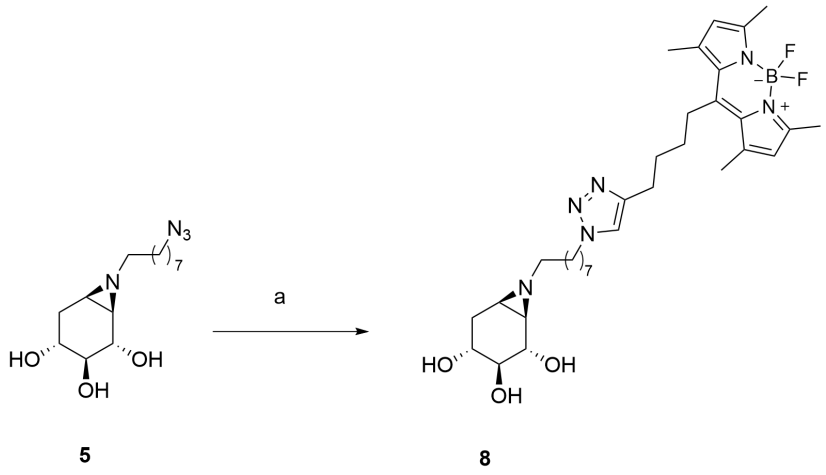

5 **8**

Scheme S1. Synthesis of β-D-*xylo*-cyclophellitol aziridine BODIPY-FL ABP **8**. Reagents and conditions: a) BODIPY tag-alkyne, $CuSO_4$, sodium ascorbate, DMF/H_2O, rt, 16 h, 58% yield.

β-D-*Xylo*-cyclophellitol aziridine BODIPY-FL ABP 8

Compound **5**[1] (4.4 mg, 14.7 µmol) was dissolved in degassed DMF (0.2 mL), then alkyne-BODIPY (1.1 eq), $CuSO_4$ (0.2 eq) and sodium ascorbate (0.4 eq) were added and the mixture stirred at rt for 16 h. The reaction mixture was concentrated and purified by semi-preparative reversed phase HPLC (linear gradient. Solutions used: A: 50 mM NH_4HCO_3 in H_2O, B: acetonitrile) yielding the desired product as an orange powder (5.4 mg, 58%).

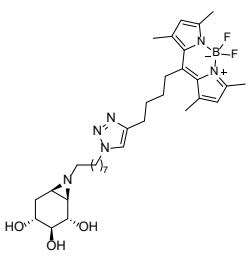

^{1}H NMR (500 MHz, CD_3OD): δ 7.73 (s, 1H), 6.11 (s, 2H), 4.35 (t, *J* = 6.9 Hz, 2H), 3.60 (d, *J* = 8.0 Hz, 1H), 3.38 (m, 1H), 3.05 (dd, *J* = 9.8, 8.0 Hz, 1H), 3.03 – 2.98 (m, 2H), 2.78 (t, *J* = 7.2 Hz, 2H), 2.44 (s, 6H), 2.38 (s, 6H), 2.30 (dd, *J* = 13.1, 5.5 Hz, 1H), 2.20 (t, *J* = 7.3 Hz, 2H), 1.92 – 1.82 (m, 5H), 1.81 – 1.77 (m, 1H), 1.68 – 1.58 (m, 3H), 1.56 (d, *J* = 6.3 Hz, 1H), 1.54 – 1.48 (m, 2H), 1.35 – 1.20 (m, 7H) ppm. ^{13}C NMR (125 MHz, CD_3OD): δ153.6, 147.2, 146.6, 140.8, 131.2, 122.0, 121.3, 77.8, 72.7, 66.8, 60.3, 49.9, 48.5, 44.0, 39.7, 32.1, 30.9, 29.9, 29.5, 29.1, 29.0, 28.5, 27.8, 26.8, 25.9, 24.6, 15.2, 13.1 ppm. HRMS (ESI) m/z: $[M+H]^+$ calculated for $C_{33}H_{49}BF_2N_6O_3$ 627.4000, found 627.4029.

Supplemental reference

1. S. P. Schröder, C. de Boer, N. G. S. McGregor, R. J. Rowland, O. Moroz, E. Blagova, J. Reijngoud, M. Arentshorst, D. Osborn, M. D. Morant, E. Abbate, M. A. Stringer, K. Krogh, L. Raich, C. Rovira, J. G. Berrin, G. P. van Wezel, A. F. J. Ram, B. I. Florea, G. A. van der Marel, J. D. C. Codée, K. S. Wilson, L. Wu, G. J. Davies and H. S. Overkleeft, Dynamic and functional profiling of xylan-degrading enzymes in aspergillus secretomes using activity-based probes, *ACS Cent. Sci.*, 2019, **5**, 1067-1078.